

## 23. STRUCTURAL ANALYSIS AND CLASSIFICATION

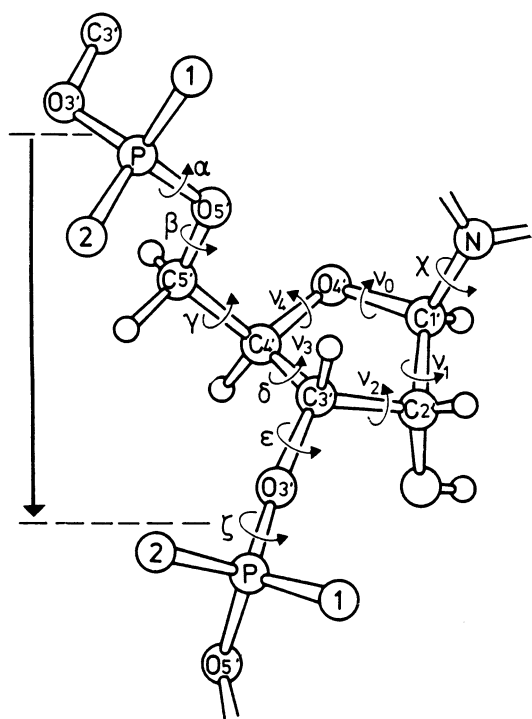


Fig. 23.3.2.2. Sugar-phosphate backbone of RNA and DNA polynucleotides. One nucleotide begins at a phosphorus atom and extends just short of the phosphorus atom of the following nucleotide, with the conventional positive direction being  $P \rightarrow O5' - C5' - C4' - C3' - O3' \rightarrow P$ , as indicated by the arrows. Main-chain torsion angles are designated  $\alpha$  through  $\zeta$ , and torsion angles about the five bonds of the ribose or deoxyribose ring are  $\nu_0$  through  $\nu_4$ , as shown. If one imagines atoms  $O3' - P - O5'$  as a hump-backed bridge, as one crosses the bridge in a positive chain direction, oxygen atom  $O1$  is to the left and  $O2$  is to the right. These oxygens, accordingly, are sometimes designated  $O_L$  and  $O_R$ . The  $-OH$  group attached to the  $C2'$  atom of the ribose ring in RNA shown here is replaced by  $-H$  in the deoxyribose ring of DNA. Atom  $N$  to the right is part of the base attached to the sugar ring:  $N1$  in pyrimidines and  $N9$  in purines. Torsion angle  $\chi$  is defined by  $O4' - C1' - N1 - C2$  in pyrimidines and  $O4' - C1' - N9 - C4$  in purines.

groups in the active sites of enzymes.) Hence, with a single-chain DNA, G-A-G-A-G-A-A-C-C-C-C-T-T-C-T-C-T-T-T-C-T-C-T-C-T-T, that folds back upon itself twice to build a triplex, NMR experiments indicate a significant amount of triplex remaining even at pH 8.0 (Sklenár & Feigon, 1990; Feigon, 1996).

## 23.3.2.4. Helix parameters

An important advantage of single-crystal oligonucleotide structures over fibre-based models is that one can actually observe local sequence-based departures from ideal helix geometry. B-DNA fibre models indicated a mean twist of *ca*  $36^\circ$  per step, or ten base pairs per turn, whereas A-DNA fibre patterns indicated less winding: *ca*  $33^\circ$  per step or 11 base pairs per turn. Twist, rise per base pair along the helix axis, horizontal displacement of base pairs off that axis, and inclination of base pairs away from perpendicularity to the axis are all intuitively obvious parameters. But when single-crystal structures began appearing in great numbers in the mid-1980s, it became imperative that uniform names and definitions be used for these and for less obvious, but increasingly significant, local helix parameters.

An EMBO workshop on DNA curvature and bending, held at Churchill College, Cambridge, in September 1988, led to an agreement on definitions and conventions that was published

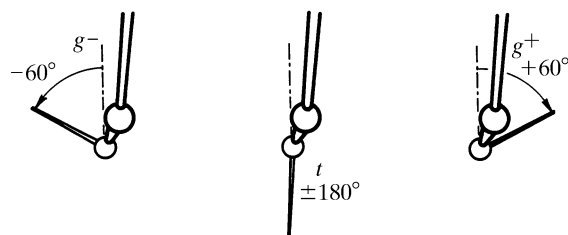


Fig. 23.3.2.3. Definition of torsion angles. A positive angle results from clockwise rotation of the farther bond, holding the nearer bond fixed. Torsion angle  $+60^\circ$  is designated as *gauche*<sup>+</sup> or  $g^+$ , angle  $180^\circ$  is *trans* or  $t$  and angle  $-60^\circ$  is *gauche*<sup>-</sup> or  $g^-$ .

simultaneously in four journals (Dickerson *et al.*, 1989). Fig. 23.3.2.10 shows the reference frames for two successive base pairs, and Figs. 23.3.2.11 and 23.3.2.12 illustrate local helix parameters involving rotation and translation, respectively. Subsequent experience has shown the most useful parameters to be inclination, propeller, twist and roll among the rotations, and  $x$  displacement, rise and slide among the translations. As mentioned at the beginning of this chapter, inclination and  $x$  displacement are the two properties that best differentiate A- from B-DNA. The four most widely used computer programs for calculation of local helix parameters are

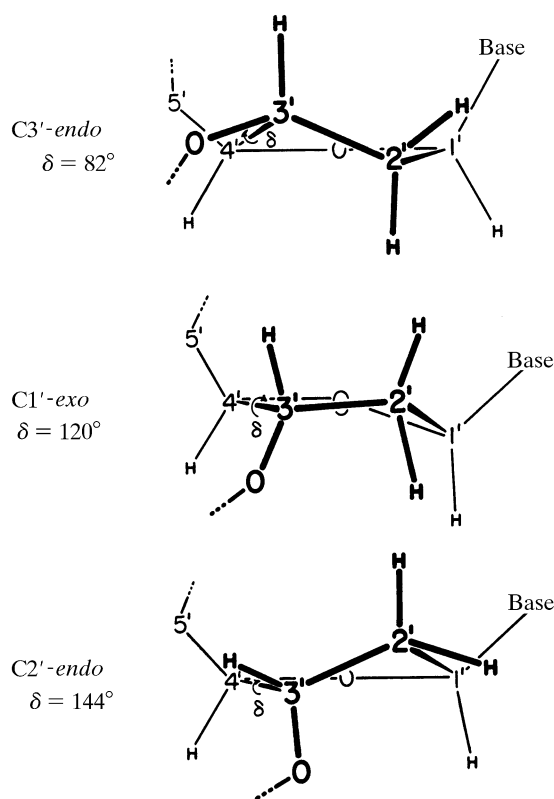


Fig. 23.3.2.4. The three most common furanose ring geometries. The planar form of the five-membered ribose or deoxyribose ring is unstable because of steric hindrance from side groups; one of the five atoms prefers to pucker out-of-plane on one side of the ring or the other. Puckering toward the same side of the ring as the  $C5'$  atom is termed *endo*, and puckering toward the opposite 'outside' surface is termed *exo*. The main-chain torsion angle  $\delta$  is related to sugar ring conformation because of the motion undergone by the  $C3' - O3'$  bond during changes in puckering.

### 23.3. NUCLEIC ACIDS

Table 23.3.2.1. Average torsion-angle properties of A-, B- and Z-DNA ( $^{\circ}$ )

Values listed are mean torsion angles, with standard deviations in parentheses. Conformations are only approximate; — indicates a non-*gauche/trans* conformation. B<sub>II</sub> and Z<sub>II</sub> are less common variants. For  $\delta$ , the sugar ring geometry is quoted in place of *gauche/trans*.  $\chi$  for B-DNA combines pyrimidines and purines. Values were obtained from a sample of 30 A-DNAs, 34 B-DNAs, 22 Z-DNAs and ten nonstandard DNAs in the Nucleic Acid Database. From Schneider *et al.* (1997).

	$\alpha$	$\beta$	$\gamma$	$\delta$	$\epsilon$	$\zeta$	$\chi$
A-DNA Conformation	293 (17) $g^-$	174 (14) $t$	56 (14) $g^+$	81 (7) C3'-endo	203 (12) $t$	289 (12) $g^-$	199 (8) $t$
B-DNA Conformation	298 (15) $g^-$	176 (9) $t$	48 (11) $g^+$	128 (13) C1'-exo	184 (11) $t$	265 (10) $g^-$	249 (16) $g^-$
B <sub>II</sub> -DNA Conformation		146 (8) —		144 (7) C2'-endo	246 (15) $g^-$	174 (14) $t$	271 (8) $g^-$
Z <sub>I</sub> -DNA – purines Conformation	71 (13) $g^+$	183 (9) $t$	179 (9) $t$	95 (8) O4'-endo	95 (8) $g^+$	301 (16) $g^-$	63 (5) $g^+$
Z <sub>II</sub> -DNA – purines Conformation					189 (12) $t$	52 (14) $g^+$	58 (5) $g^+$
Z <sub>I</sub> -DNA – pyrimidines Conformation	201 (20) $t$	225 (16) —	54 (13) $g^+$	141 (8) C2'-endo	267 (9) $g^-$	75 (9) $g^+$	204 (98) $t$
Z <sub>II</sub> -DNA – pyrimidines Conformation	168 (16) $t$	166 (14) $t$					

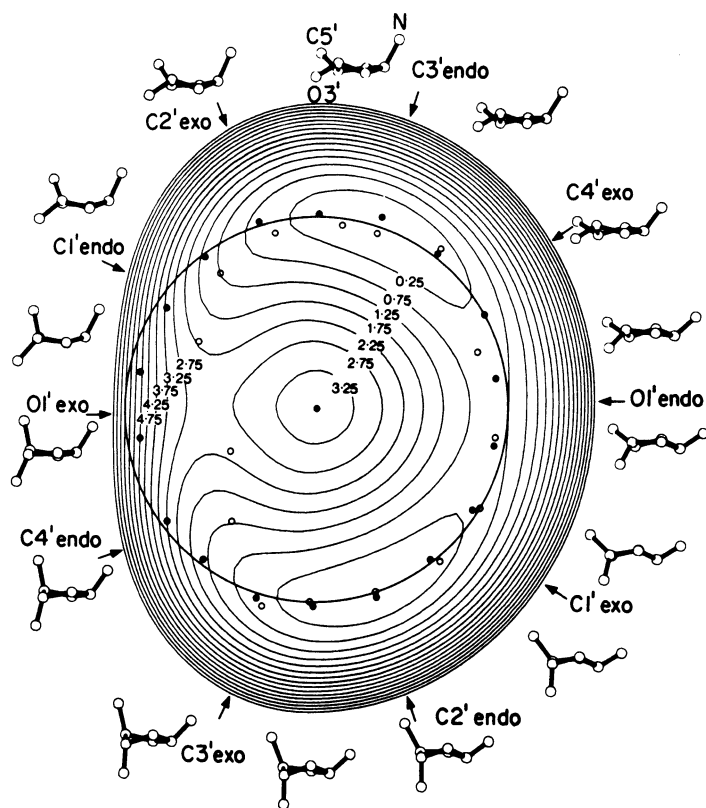


Fig. 23.3.2.5. Potential plot of all furanose ring conformations. Energies are in kcal mol<sup>-1</sup>. The distance from the central point gives the maximum displacement of the out-of-plane atom from the plane of the other four. The circle is a constant-displacement trajectory chosen to pass through the potential minima on the right three-quarters of the plot. C2'-endo and C3'-endo are especially favoured, whereas O1'-exo on the left is highly disfavoured. The path from C2'-endo through C1'-exo, O1'-endo and C4'-exo to C3'-endo is a low-energy path, and many examples all along this path are known in B-DNA helices. Reprinted with permission from Levitt & Warshel (1978). Copyright (1978) American Chemical Society.

Table 23.3.2.2. Sugar ring conformations, pseudorotation angles and torsion angle  $\delta$

Ring conformation	Pseudorotation angle ( $^{\circ}$ )	Torsion angle $\delta$ ( $^{\circ}$ )
C3'-endo	18	82
C4'-exo	54	82
O4'-endo	90	96
C1'-exo	126	120
C2'-endo	162	144
C3'-exo	198	158
C4'-endo	234	158
O4'-exo	270	144
C1'-endo	306	120
C2'-exo	342	96

*NEWHELIX* by Dickerson (B7, B46), *CURVES* by Lavery & Sklenar (1988, 1989), *BABCOCK* by Babcock & Olson (Babcock *et al.*, 1993, 1994; Babcock & Olson, 1994) and *FREEHELIX* (Dickerson, 1998c). *NEWHELIX* was the earliest of these, but it performs all calculations relative to a best overall helix axis. This is satisfactory for single-crystal DNA structures, but makes the program unusable for the 180° bending observed in some protein–DNA complexes. *CURVES* is especially convenient for mapping the axis of a bent or curved helix. *FREEHELIX*, which evolved from *NEWHELIX*, calculates all parameters relative to local base-pair geometry, without assuming an overall axis, and permits display of normal vector plots that are especially useful in analysing bending in DNA–protein complexes (Dickerson & Chiu, 1997).